genes

MDPI

Article

Transcriptomic Profiling Reveals Porcine IFI35 as a Restriction Factor Against H1N1 Swine Influenza Virus and the Antagonism of IFI35 by Viral NS1

Yongbo Liu [1], Xiangyue Xie [1], Zhen Wang [2] and Shaotang Ye [3,*]

[1] Hebei Key Laboratory of Veterinary Preventive Medicine, College of Animal Science and Technology, Hebei Normal University of Science & Technology, Qinhuangdao 066000, China; lyb4139@hevttc.edu.cn (Y.L.); xxy4178@hevttc.edu.cn (X.X.)
[2] College of Veterinary Medicine, South China Agricultural University, Guangzhou 510642, China; zhenwang@outlook.com
[3] College of Animal Sciences, Zhejiang University, Hangzhou 310058, China
* Correspondence: 0625c52@zju.edu.cn

Abstract

Background/Objectives: Influenza A virus (IAV) poses a persistent threat to the swine industry and public health, and host restriction factors in pigs remain insufficiently characterized. This study investigated whether porcine interferon-induced protein 35 (IFI35) restricts H1N1 swine influenza virus (SIV) replication and how the viral NS1 protein counteracts this defense. Methods: Porcine IFI35 was overexpressed in PK-15, HEK293T, and MDCK cells followed by H1N1 SIV infection; cytopathic effects, viral NP levels, and viral titers were assessed. RNA-seq and qPCR were used to profile and validate host transcriptional responses. The effect of NS1 on RIG-I-like receptor (RLR) signaling was examined by Western blotting. Results: IFI35 overexpression attenuated SIV-induced cytopathic effects and reduced viral NP levels and titers. Transcriptomics revealed that IFI35 reshaped the host transcriptome, enriching antiviral, RLR, and NOD-like receptor pathways, and upregulated *IFNB1*, *IFNE*, *MDA5*, and interferon-stimulated genes; SIV infection counteracted these changes and downregulated endogenous *IFI35*, an effect associated with the viral NS1 protein. NS1 reduced MDA5, RIG-I, and MAVS protein levels. Conclusions: Porcine IFI35 restricts H1N1 SIV and is antagonized by NS1 through combined transcriptional suppression and RLR pathway blockade, revealing an IFN-ε-associated defense axis and candidate antiviral targets in the swine host.

Keywords: porcine IFI35; H1N1 subtype; NS1 antagonism; RIG-I-like receptor signaling; interferon epsilon; transcriptome profiling

Check for updates

Academic Editor: Robert L. Taylor

Received: 20 September 2026
Revised: 30 October 2026
Accepted: 12 November 2026
Published: 18 November 2026

Copyright: © 2026 by the authors. Licensee MDPI, Basel, Switzerland. This article is an open access article distributed under the terms and conditions of the Creative Commons Attribution (CC BY) license.

1. Introduction

Swine influenza (SI) is a widespread respiratory disease in pigs that is endemic in major swine-producing regions globally. It is caused by influenza A virus (IAV), a member of the Orthomyxoviridae family. This enveloped, negative-sense, single-stranded segmented RNA virus, characterized by its capacity to undergo antigenic drift and shift, poses substantial challenges to global public health due to its interspecies transmissibility and pandemic potential [1]. The H1N1 subtype of swine influenza virus (H1N1 SIV), recognized for its zoonotic potential, emerged as a significant global health concern during the 2009 pandemic [2]. SIV infection commonly causes high morbidity (up to 100%) but low mortality in infected pig herds; however, mortality rates can escalate to 10–15% in naïve pigs [3].

Clinical manifestations in infected pigs primarily include fever, sneezing, nasal discharge, coughing, and weight loss. Although the direct mortality rate associated with SIV infection is relatively low, the virus impairs the host immune system, thereby drastically increasing susceptibility to secondary infections by other pathogens and causing severe economic losses to the swine industry [4]. The complex interplay between the viral genome and host factors, particularly the innate immune response, dictates the course of infection and disease severity [5]. While SIV was historically considered a seasonal pathogen similar to human influenza viruses, the modern, highly centralized swine farming model enables continuous viral circulation and transmission throughout the year [6]. Amidst the continuous evolution of this zoonotic virus, understanding the molecular mechanisms of pathogenesis and host immune responses has become paramount. Despite advancements in vaccine development and antiviral therapies, the host factors that restrict SIV replication in porcine cells remain incompletely understood [7].

The host innate immune response serves as the first line of defense against viral infection and plays a crucial role in monitoring viral invasion and rapidly initiating antiviral programs. Central to this defense system is the activation of pattern recognition receptors (PRRs), such as Toll-like receptors (TLRs) and retinoic acid-inducible gene I (RIG-I)-like receptors (RLRs), which recognize specific viral components and trigger signaling cascades leading to the production of pro-inflammatory cytokines and type I interferons (IFNs) [8,9]. During the early stages of infection, viruses inevitably trigger host innate immune surveillance, which initiates a robust antiviral response. In response, these viruses have evolved sophisticated immune evasion strategies to suppress host antiviral response mediators, particularly type I IFNs [10–12]. Interferon-stimulated genes (ISGs) serve as the primary effectors of the IFN response, playing essential roles in host defense against microbial infections [13,14]. Although hundreds of ISGs have been identified since their discovery, the antiviral spectrum, target specificity, and mechanisms of most ISGs remain poorly defined.

As a prominent member of the ISG family, IFN-induced protein 35 (IFI35, also known as IFP35) is a 35 kDa protein initially identified via cDNA library screening of IFN-γ-stimulated HeLa cells [15]. IFI35 possesses an atypical leucine zipper domain. Although it lacks the basic structural domain necessary for direct nucleic acid binding, its N-terminal domain (NID) can bind to pathogen-specific components to form homodimers and heterodimers, or interact with N-myc-interacting protein (Nmi) to form high-molecular-mass complexes (HMMCs) of 200 to 400 kDa through which IFI35 exerts its antiviral activity [16,17]. As an interferon-inducible protein, IFI35 has been reported to negatively regulate RIG-I-mediated antiviral signaling in certain contexts, thereby facilitating the replication of vesicular stomatitis virus (VSV) [18]. Conversely, IFI35 has been demonstrated to effectively inhibit the replication of foot-and-mouth disease virus [19] and bovine foamy virus [20]. The IAV nonstructural protein NS1 is the principal viral antagonist of host innate immunity, suppressing type I IFN induction through interactions with RIG-I and TRIM25 [21]. Notably, Yang et al. demonstrated that human IFI35 engages in mutual antagonism with IAV NS1 in human cells [22]; however, whether this antagonistic axis operates in the natural swine host—where IFI35 sequence divergence and SIV-specific NS1 variants may alter the interaction—has not been examined. Intriguingly, IFI35 exhibits strain-specific phenotypes: it inhibits H3N2 IAV replication but reportedly promotes H7N9 infection [22]. These contrasting findings indicate that IFI35 can exert diverse effects on the host response depending on the specific invading virus. However, whether porcine IFI35 can restrict the replication of H1N1 SIV and how it modulates host interferon responses during SIV infection remain largely unknown.

Due to the strong strain and host specificity exhibited by IFI35 during influenza virus infection, in this study, we evaluated the antiviral activity of porcine IFI35 against H1N1 SIV in vitro. Subsequently, transcriptomic analysis was employed to characterize comprehen-

sively how porcine IFI35 reshapes host innate immunity. We also examined NS1-mediated antagonism of the host antiviral response, including the suppression of key proteins in the RLR signaling pathway. This study elucidates the specific contributions of IFI35 to the host antiviral defense network against SIV, providing insights into novel therapeutic targets and the development of immuno-modulatory strategies against SIV infection.

2. Materials and Methods

2.1. Cells, Viruses, Plasmids, Antibodies and Virus Titration

Human embryonic kidney (HEK) 293T cells, Madin–Darby canine kidney (MDCK) cells and porcine kidney 15 (PK15) cells were cultured at 37 °C and 5% (*v*/*v*) CO_2 in Dulbecco's modified Eagle medium (DMEM; Biological Industries, Kibbutz Beit-Haemek, Israel) supplemented with 10% fetal bovine serum (Biological Industries, Kibbutz Beit-Haemek, Israel). The H1N1 SIV strain (A/Swine/Guangdong/YJ4/2014) was kindly provided by Professor Zhang Guihong at South China Agricultural University (Guangzhou, China). Sendai virus (SeV) was maintained in our laboratory. Plasmids used in this study included pCAGGS-HA-poIFI35 (HA-tagged porcine IFI35), pEGFP-poIFI35 (GFP-tagged porcine IFI35), pEGFP-NS1 (GFP-tagged SIV NS1) and pNS1-mCherry (mCherry-tagged SIV NS1). The porcine IFI35 sequence (GenBank: XM_003358024.4) was cloned into pEGFP-C1 to generate pEGFP-poIFI35, encoding an N-terminal GFP-tagged fusion protein. The NS1 coding sequence of H1N1 SIV (strain A/Swine/Guangdong/YJ4/2014) was amplified from viral cDNA and cloned into pmCherry-C1 to generate pNS1-mCherry, encoding an N-terminal mCherry-tagged fusion protein. All constructs were verified by sequencing. Antibodies included Goat anti-mouse IgG (H&L) Alexa Fluor 680 (AB175775, Abcam, Cambridge, UK), Goat anti-Rabbit IgG (H&L) Alexa Fluor 790 (AB175781, Abcam, Cambridge, UK), α-tubulin (AB7291, Abcam, Cambridge, UK), GAPDH antibody (GTX100118, GeneTex, Irvine, CA, USA), β-actin antibody (GTX109639, GeneTex, Irvine, CA, USA), GFP tag antibody (GTX628528, GeneTex, Irvine, CA, USA), mCherry tag antibody (GTX128508, GeneTex, Irvine, CA, USA), MAVS antibody (GTX32966, GeneTex, Irvine, CA, USA), Influenza A virus NP antibody (GTX125989, GeneTex, Irvine, CA, USA), Influenza A virus M1 antibody (GTX125928, GeneTex, Irvine, CA, USA), RIG-I antibody (67556-1, Proteintech, Wuhan, China) and MDA5 antibody (21775-1, Proteintech, Wuhan, China). The virus was stored at −80 °C until use; the titer was determined as log10 (median tissue culture infectious dose [$TCID_{50}$]/mL) and calculated using the Reed–Muench method as previously described [23].

2.2. Cell Transfection and Virus Infection

PK-15, MDCK, or HEK293T cells were inoculated in culture vessels prior to transfection. When the cells reached 80% confluence, according to the manufacturer's instructions, we used Lipofectamine 3000 (40801ES01, Yeasen, Shanghai, China) to transfect the cells with 2.5 μg pCAGGS-HA-poIFI35 or pEGFP-poIFI35. Empty vector (pEGFP or pCAGGS-HA)-transfected cells served as negative controls. Then, 24 h after transfection, cells were infected with H1N1 SIV at the specified multiplicity of infection (MOI; 0.1 or 2.0). For NS1 overexpression studies, PK15 cells were transfected with pEGFP-NS1 or pNS1-mCherry (2.5 μg) for 24 h prior to RNA harvesting or Sendai virus (SeV) infection. For siRNA-mediated knockdown, PK15 cells were transfected with gene-specific siRNAs (sequences listed in Supplementary File S1) for 48 h and subsequently infected with H1N1 SIV (MOI = 0.1) for 24 h. For RIG-I-like receptor pathway activation, SeV was inoculated into PK15 cells at an MOI of 1.0 for 12 h prior to protein harvest.

2.3. RNA Extraction, cDNA Synthesis, and Quantitative PCR (qPCR)

The total RNA extraction from cells, cDNA synthesis and qPCR tests were performed as previously described [23]. Primer sets used for qPCR are listed in Supplementary File S1.

2.4. Western Blotting

Cells derived from samples were lysed using cell lysis buffer for Western blotting (Beyotime, Shanghai, China). Cell lysates were collected and centrifuged at 15,000× *g* for 10 min at 4 °C. The protein concentration was determined using a BCA protein assay kit (Beyotime, Shanghai, China). Equal amounts of protein (30 μg) were subjected to SDS-PAGE and transferred to a PVDF membrane. The membranes were washed with PBS and then blocked with QuickBlock Blocking Buffer for Western blotting (Beyotime) at room temperature, and then incubated overnight at 4 °C with the indicated primary antibodies. After washing with PBST (PBS with 0.1% Tween-20), the secondary antibodies were incubated for 1 h at room temperature on the orbital shaker. Protein bands were visualized by Odyssey Sa (Li-COR, Lincoln, NE, USA) and analyzed by Image Studio version 4.0 software (Li-COR).

2.5. Construction of RNA Sequencing Libraries, Sequencing and Data Analysis

The PK15 cells were transfected with 2.5 μg HA-tagged porcine IFI35. Three independent biological replicates per group were used. Empty vector (pCAGGS-HA)-transfected cells served as controls. Cells were infected with H1N1 SIV at 1 multiplicity of infection (MOI) for 48 h. The total RNA of these cells was extracted and used for the next step. The cDNA libraries were produced by the VAHTS Universal V6 RNA-seq Library Prep Kit (Vazyme, Nanjing, China) according to the manufacturer's instructions. The purified and enriched cDNA libraries were quantified by Agilent 2200 TapeStation (Agilent Technologies, Santa Clara, CA, USA), and the cDNA libraries were sequenced by DNBSEQ-T7 (MGI Tech, Shenzhen, China).

2.6. Functional Annotation, Classification and Differential Gene Expression Analysis

Before read mapping, clean reads were obtained from the raw reads by removing the adaptor sequences and low-quality reads. The clean reads were used for subsequent analysis. Clean reads were aligned to the Sus scrofa reference genome (Sscrofa11.1) using HISAT2 (v2.2.1); gene-level counts were obtained with HTSeq (v0.11.2), and the RPKM method was used to determine the gene expression levels. The unique reads were analyzed by the DESeq2 (version 1.42.0) algorithm to filter the differentially expressed genes (DEGs). Significance was assessed with the following criteria: $|\log2(\text{fold change})| \geq 0.585$ and Benjamini–Hochberg adjusted $p < 0.05$. The DEGs are listed in Supplementary File S2.

2.7. Gene Ontology and Pathway Enrichment Analysis

To analyze the DEGs, Fisher's exact test was applied for the Gene Ontology (GO) analysis to elucidate the biological implications ($p < 0.05$), including molecular function, cellular component, and biological process. Additionally, Fisher's exact test was also used for the Kyoto Encyclopedia of Genes and Genomes (KEGG) signaling pathways analysis ($p < 0.05$). The details of GO and pathway enrichment analyses are listed in Supplementary File S3 and Supplementary File S4, respectively.

2.8. RNA Interference

As described in our previous study [23], the PK15 cells were transfected with siRNA for 48 h. Then the cellular RNA was obtained and used for subsequent cDNA synthesis and qPCR. The sequences of siRNAs are listed in Supplementary File S1.

2.9. Statistical Analysis

Statistical analyses were performed using GraphPad Prism version 10.3 (GraphPad Software, San Diego, CA, USA). Comparisons between two groups were performed using an unpaired two-tailed Student's *t*-test; comparisons among three or more groups were performed using one-way ANOVA followed by Tukey's multiple-comparison test. Viral growth kinetics were analyzed by two-way ANOVA followed by Šídák's multiple-comparison test. Data are presented as mean ± SD from at least three independent experiments. * $p < 0.05$, ** $p < 0.01$, *** $p < 0.001$, **** $p < 0.0001$.

3. Results

3.1. Overexpression of Porcine IFI35 Attenuated H1N1 SIV-Induced CPE and Restricted Viral Replication

IFI35 has been reported to exert differential effects on different influenza virus subtypes [22]; however, the impact of porcine IFI35 on H1N1 SIV remains unknown. To evaluate the effect of porcine IFI35 on H1N1 SIV, we overexpressed porcine IFI35 in PK15 cells and subsequently infected them with H1N1 SIV, after which we monitored the resulting cytopathic effects (CPE). PK15 cells were used as a porcine host-cell model; HEK293T and MDCK cells, which support higher transfection efficiency and viral replication, respectively, were used to corroborate the findings. The results showed that empty vector-transfected PK15 cells displayed severe CPE, characterized by prominent cell rounding, shrinkage, clustering, and detachment (Figure 1A). In contrast, PK15 cells overexpressing porcine IFI35 showed markedly attenuated CPE, with only mild shrinkage and slight clumping observed. These findings indicated that porcine IFI35 overexpression significantly alleviated H1N1 SIV-induced cellular damage, consistent with the reduced viral protein levels and lower viral titers shown in Figure 1B,C. To confirm the effect of porcine IFI35 on H1N1 SIV replication efficiency, we overexpressed porcine IFI35 in HEK293T cells, which have higher transfection efficiency, and evaluated the level of SIV NP protein in cell lysates following H1N1 SIV infection by Western blotting. The results demonstrated that SIV NP protein expression was significantly reduced in the lysates of IFI35-overexpressing cells compared to the control group (Figure 1B), indicating that porcine IFI35 overexpression markedly suppressed H1N1 SIV replication in HEK293T cells. To further validate this, we measured viral titers in MDCK cells (higher replication efficiency) overexpressing porcine IFI35 at different time points after infection with H1N1 SIV. Consistent with the previous results, the viral titers of SIV were significantly reduced in MDCK cells overexpressing porcine IFI35 (Figure 1C). These results demonstrated that overexpression of porcine IFI35 in host cells attenuated H1N1 SIV replication.

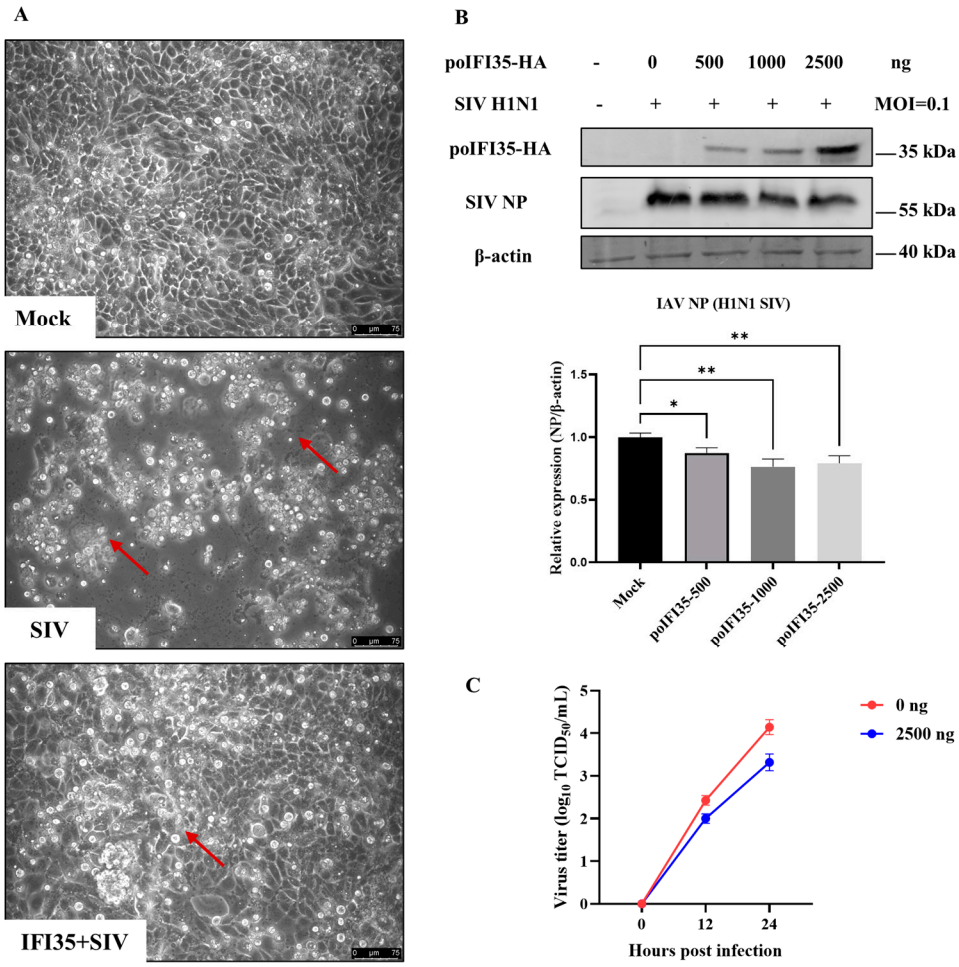


Figure 1. Overexpression of porcine IFI35 inhibited H1N1 SIV replication. (**A**) bright-field observations of PK15 cells with different treatments (×400). Cells were infected for 24 h at 2 MOI. The arrow indicates the cytopathic effect. (**B**) HEK293T cells overexpressing porcine IFI35 were infected with H1N1 SIV for 24 h at 0.1 MOI. The protein bands were subjected to densitometric analysis relative to the reference protein β-actin as a loading control. (**C**) H1N1 SIV growth kinetics monitored over 24 h in MDCK cells transfected with poIFI35–HA or empty vector. ($n = 3$, * $p < 0.05$, ** $p < 0.01$).

3.2. Differential Gene Expression Analysis of Overexpression of Porcine IFI35 in Non-Infected and SIV-Infected PK15 Cells

To characterize host transcriptional changes associated with IFI35-mediated restriction of SIV replication, transcriptome analysis was carried out in this study. We used DESeq software to calculate the fold change (FC) values of each gene in the overexpression group or infection group compared to the control group. The results showed that 2621 (IFI35_vs_Mock), 4138 (SIV_vs_Mock), 3527 (IFI35-SIV_vs_Mock), and 888 (IFI35-SIV_vs_SIV) differentially expressed genes (DEGs) were identified in different comparison groups (Figure 2). Among them, DEG analysis of the comparative groups (IFI35_vs_Mock, SIV_vs_Mock, IFI35-SIV_vs_Mock, and IFI35-SIV_vs_SIV) identified 1254, 2192, 1791, and 366 upregulated genes and 1367, 1946, 1736, and 522 downregulated genes, respectively (Figure 2). Notably, comparison of SIV-infected PK15 cells with and without IFI35 overexpression (IFI35-SIV vs. SIV) identified 888 DEGs, comprising 366 upregulated and 522 downregulated genes, indicating that porcine IFI35 substantially reshaped the host transcriptional landscape to restrict SIV replication.

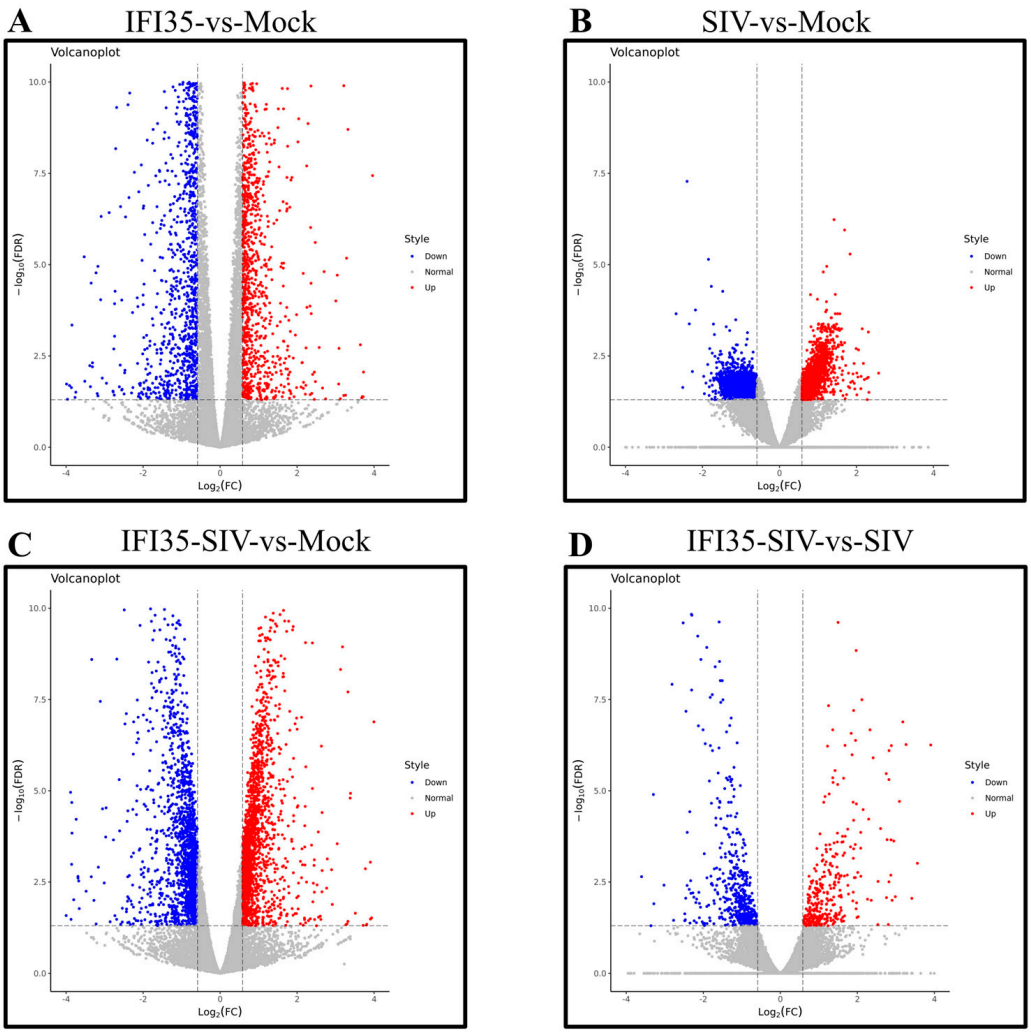


Figure 2. Volcano plots of differentially expressed genes (DEGs; |log2FC| ≥ 0.585, adjusted $p < 0.05$) in (**A**) IFI35 vs. mock, (**B**) SIV vs. mock, (**C**) IFI35 + SIV vs. mock, and (**D**) IFI35 + SIV vs. SIV ($n = 3$ per group). Red and blue dots denote up- and downregulated genes, respectively. The vertical dashed lines indicate a $|\log_2(\text{fold change})|$ of 1, and the horizontal dashed line indicates a p-value of 0.05 ($-\log_{10}(p) = 1.3$). Blue and red dots represent down- and up-regulated genes, respectively, and gray dots represent non-significant genes.

3.3. Gene Ontology and Pathway Enrichment Analysis of Overexpression of Porcine IFI35 in Non-Infected and SIV-Infected PK15 Cells

To further unveil the unique insights of IFI35 limiting SIV replication, the DEGs were analyzed and classified by Gene Ontology (GO) enrichment and pathway enrichment. The DEGs in the comparative group IFI35_vs_Mock mainly involved biological processes and were related to antiviral immunity, such as viral genome replication, RIG-I-like receptor signaling pathway, JAK-STAT signaling pathway, NOD-like receptor signaling pathway, Toll-like receptor signaling pathway and IL-17 signaling pathway (Figure 3A). The DEGs in the comparison group SIV_vs_Mock were associated with DNA damage repair, protein modification and innate immune response, such as cellular response to DNA damage stimuli, DNA repair, regulation of DNA replication, protein ubiquitination and deubiquitination, and the RIG-I-like receptor signaling pathway (Figure 3B). The DEGs in the comparative group IFI35-SIV_vs_Mock were associated with viral genome replication and antiviral immunity, such as regulation of the apoptotic process, negative regulation of viral genome replication, cellular response to DNA damage stimuli, response to IFNs, regulation of the

RIG-I signaling pathway and NOD-like receptor signaling pathway, C-type lectin receptor signaling pathway, and IL-17 signaling pathway (Figure 4A). Importantly, most DEGs in the IFI35-SIV_vs_SIV comparison group were associated with viral replication and antiviral immunity, such as defense response to virus, negative regulation of viral genome replication, and NOD-like receptor signaling pathway (Figure 4B). Consistently, pathway enrichment analysis showed that the DEGs were enriched in antiviral and innate immune-related pathways, including the RIG-I-like receptor, JAK-STAT, NOD-like receptor, Toll-like receptor, C-type lectin receptor, and IL-17 signaling pathways (Figure 5A–D).

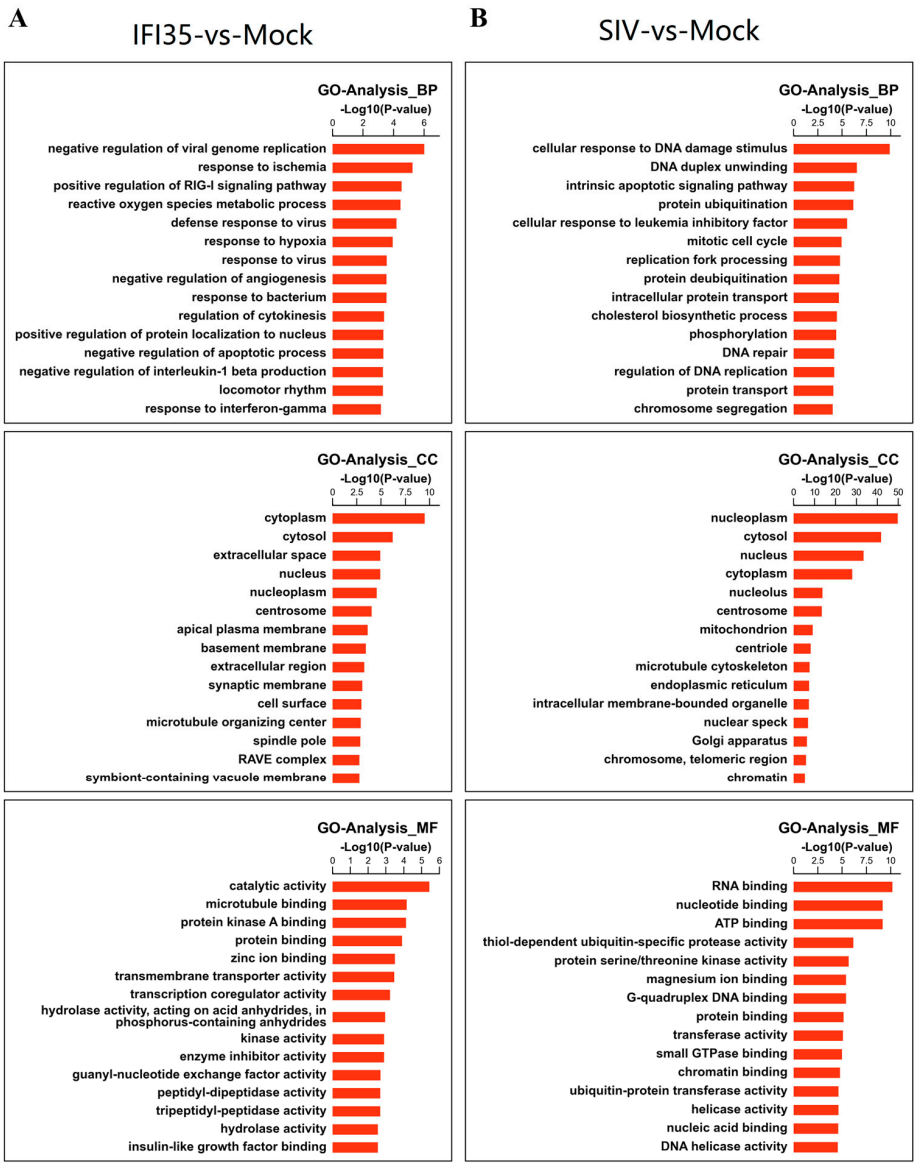


Figure 3. GO enrichment analysis of DEGs in (**A**) IFI35 vs. mock and (**B**) SIV vs. mock ($n = 3$ per group). Bubble size represents gene count; color intensity represents −log10 (adjusted p-value).

3.4. Overexpression of Porcine IFI35 Modulated the Transcription of Innate Immunity-Related Genes in PK15 Cells

GO and KEGG enrichment analyses suggested that the overexpression of porcine IFI35 and SIV infection both regulated the host cell's innate immune response. To further validate this, we performed quantitative PCR. The results demonstrated that overexpression of porcine IFI35 upregulated the transcription of porcine genes *IFNB1*, *IFNE*, *MDA5*,

ISG15, *OAS1* and *OAS2*. Moreover, we observed that following SIV infection of IFI35-overexpressing cells, the mRNA levels of these IFI35-induced genes (except *OAS2*) were suppressed upon SIV infection, suggesting a potential counter-regulatory effect of SIV infection on IFI35-induced gene transcription (Figure 6A–F). Interestingly, in the absence of IFI35 overexpression, SIV infection induced *IFNE* but not *IFNB1* transcription; however, SIV infection attenuated the stronger induction of both genes driven by IFI35 overexpression (Figure 6A,B). Additionally, to validate the effect of SIV on IFI35 gene transcription, we infected PK15 cells with H1N1 SIV and assessed *IFI35* mRNA expression in cell lysates. The qPCR demonstrated that SIV infection significantly downregulated IFI35 transcription (Figure 6G). These data demonstrated that porcine IFI35 modulated the transcription of innate immunity-related genes in PK15 cells; however, SIV infection suppressed porcine *IFI35* transcription. Whether SIV antagonizes IFI35-triggered innate immune responses through this pathway remains to be further investigated.

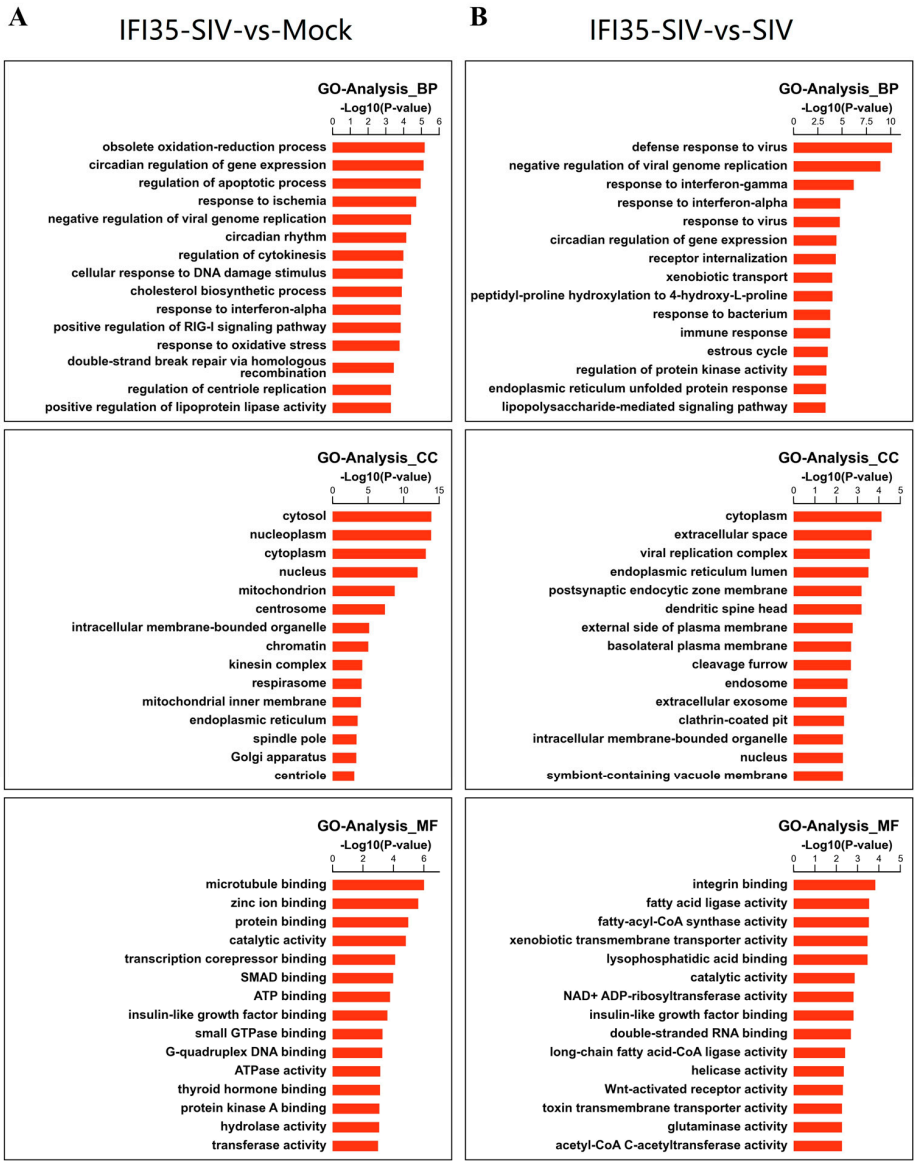


Figure 4. Gene Ontology enrichment analysis of different groups. (**A**) indicates the IFI35 + SIV vs. mock group. (**B**) indicates the IFI35 + SIV vs. SIV group.



Figure 5. Pathway enrichment analysis of different groups. (**A**) indicates the IFI35 vs. mock group. (**B**) indicates the SIV vs. mock group. (**C**) indicates the IFI35 + SIV vs. mock group. (**D**) indicates the IFI35 + SIV vs. SIV group.

3.5. SIV NS1 Suppresses Porcine IFI35-Associated Antiviral Transcription and RLR Signaling

The non-structural protein NS1 of IAV is a multifunctional antagonist of the host immune response. To further elucidate the potential mechanism by which SIV-induced antagonism suppresses porcine IFI35 transcription, we evaluated the expression of *IFNE*, *IFI35*, and *MDA5* in NS1-overexpressing PK15 cells. The qPCR showed that SIV NS1 suppressed the transcription of *IFNE*, *IFI35*, and *MDA5* (Figure 7A–C), suggesting that the SIV-mediated downregulation of *IFI35* transcription is closely associated with NS1. To assess the roles of *IFNE*, *IFI35*, and *MDA5* in SIV replication, we examined SIV replication efficiency in PK15 cells individually silenced for *IFNE* (Figure 7D), *MDA5* (Figure 7E), or *IFI35* (Figure 7F). The results showed that siRNA-mediated silencing of all three genes significantly promoted SIV replication (Figure 7G). These results suggest that NS1 counteracts the host antiviral barrier by suppressing the transcription of *IFI35*, *MDA5*, and *IFNE*, thereby weakening the host restriction barrier and facilitating viral replication.

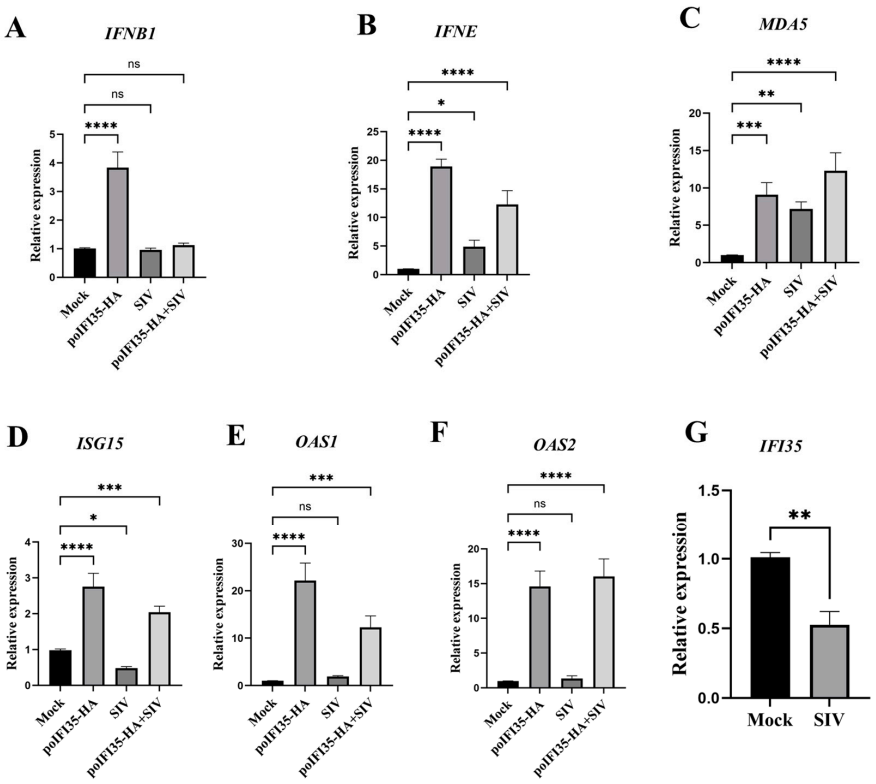


Figure 6. Regulation of gene transcription by IFI35 overexpression and SIV infection. (**A**–**F**) indicate the transcriptional levels of genes *IFNB1*, *IFNE*, *MDA5*, *ISG15*, *OAS1* and *OAS2*. (**G**) indicates the suppression of porcine IFI35 transcription by SIV infection. (ns indicates no significance, * $p < 0.05$, ** $p < 0.01$, *** $p < 0.001$, **** $p < 0.0001$).

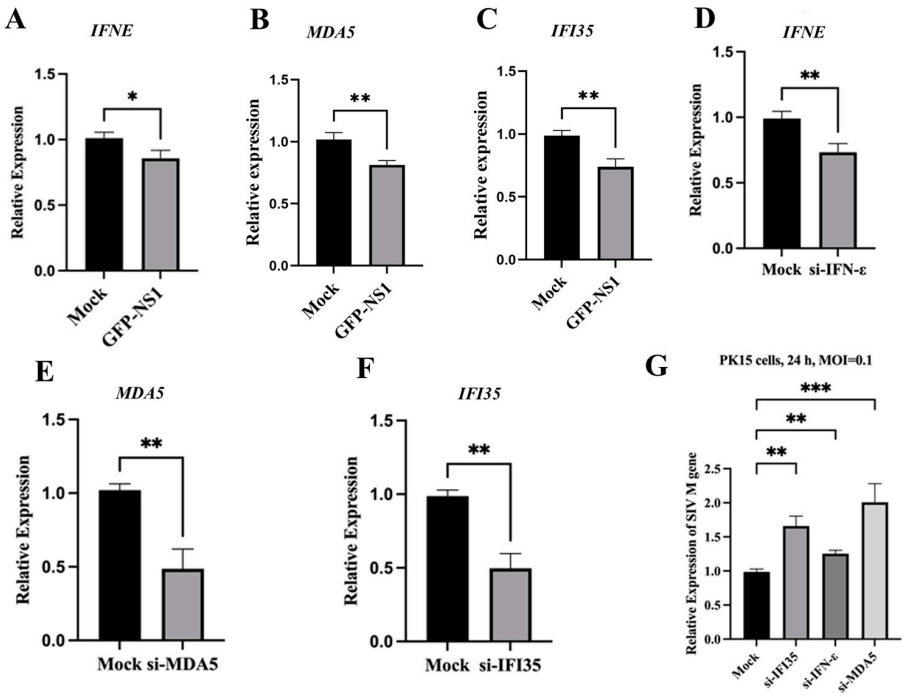


Figure 7. Antagonistic effect of NS1 and RNAi validation. (**A**–**C**) indicate the suppression of the porcine *IFNE*, *IFI35* and *MDA5* transcription by the SIV NS1. (**D**–**F**) indicate the RNA interference efficiency of siRNA. (**G**) indicates the effect of RNA interference on SIV infection (* $p < 0.05$, ** $p < 0.01$, *** $p < 0.001$).

3.6. SIV NS1 Suppresses Key Proteins of the RLR Signaling Pathway

To evaluate the general inhibitory effect of NS1 on the RLR pathway, we employed a classical RLR pathway activation model (induced by SeV). Western blotting revealed that the overexpression of SIV NS1 significantly reduced the protein expression of porcine MDA5, RIG-I, and MAVS induced by SeV (Figure 8). These results indicate that SIV NS1 antagonizes the host antiviral response by suppressing key protein components of the RLR signaling pathway.

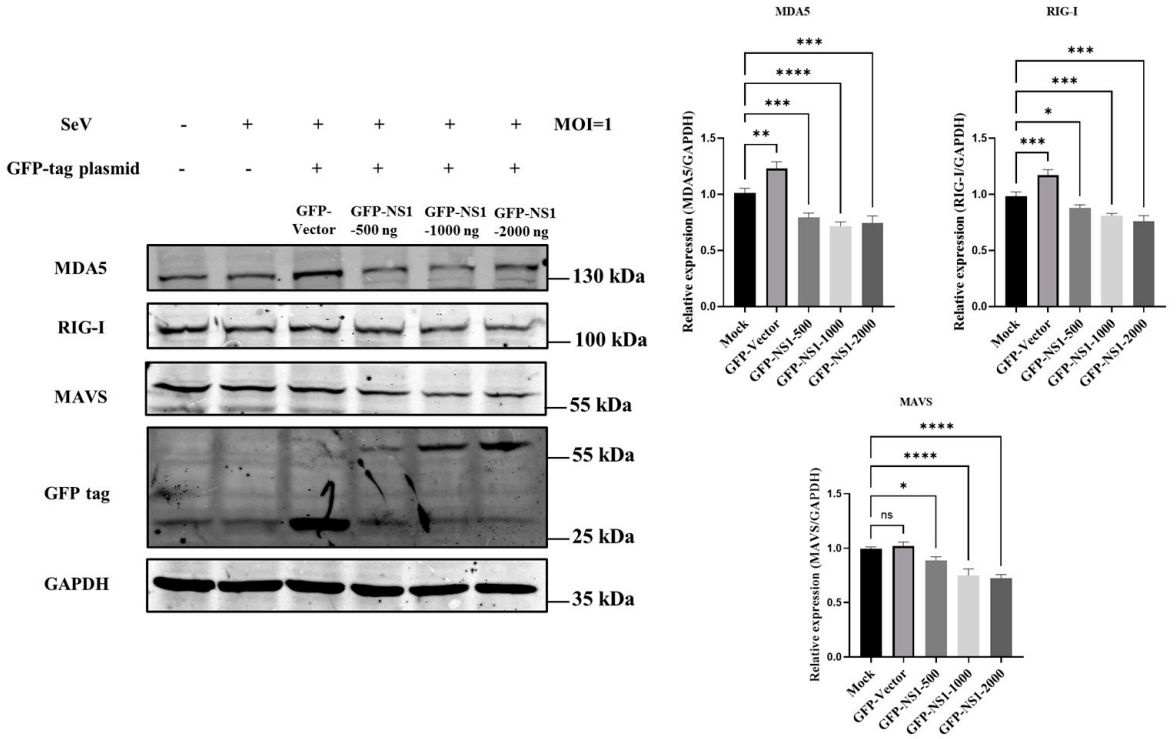


Figure 8. SIV NS1 inhibited the expression of key proteins in the Sendai virus (SeV)-induced RIG-I-like signaling pathway. Western blotting analysis of RLR signaling proteins (MDA5, RIG-I, and MAVS) in PK15 cells transfected with SIV NS1 and subsequently induced by SeV. Protein bands were normalized to GAPDH. (ns indicates no significance, * $p < 0.05$, ** $p < 0.01$, *** $p < 0.001$, **** $p < 0.0001$).

4. Discussion

SIV continues to actively circulate and evolve within global pig populations. Its ability to breach species barriers and cause direct human infections, as highlighted by the 2009 pandemic, underscores its public health significance [24]. Surveillance data indicate that three primary subtypes of IAV, H1N1, H3N2, and H1N2, are concurrently circulating in swine herds worldwide [7,25]. The evolution of these viruses is driven by mechanisms such as antigenic drift and shift, leading to the emergence of new strains. Consequently, understanding the host–pathogen interaction mechanisms is critical for developing broad-spectrum vaccines and therapeutic targets.

A major finding of our study is the atypical induction of IFN-ε and MDA5 driven by porcine IFI35. Type I IFNs, which include IFN-α/β/ω/κ/ε/δ/τ/ν/ζ, are key effectors of innate antiviral immunity. Among these, IFN-α/β exert antiviral effects against IAVs [26]. Interestingly, while previous studies suggested that porcine IFN-ε exhibits limited antiviral efficacy against viruses like PRRSV [27,28], our datasets revealed IFI35-driven upregulation of both *IFNB1* and *IFNE* in uninfected cells, whereas SIV infection induced *IFNE* but not *IFNB1*. Unlike other type I IFNs, IFN-ε exhibits significantly weaker antiviral activity than IFN-α; it is constitutively expressed in mucosal tissues and serves as an important comple-

ment to innate immunity [29]. We hypothesize that porcine IFI35 is associated with the induction of IFN-ε and MDA5, suggesting a potential IFN-ε-linked mucosal defense that compensates for the rapid SIV-mediated suppression of IFN-α/β during the early phase of infection. The causal contribution of the IFN-ε/MDA5 to IFI35-mediated restriction, however, remains to be established. Because IFN-ε was assessed only at the transcriptional level, its functional contribution was not pursued further in this study. The upregulation of IFN-ε, MDA5, and downstream ISGs (ISG15, OAS1, and OAS2) following porcine IFI35 overexpression indicates that porcine IFI35 is associated with the transcriptional upregulation of innate immune genes. This immune activation broadens our current understanding of type I IFNs in swine respiratory infections, highlighting a novel regulatory axis driven by porcine IFI35.

Moreover, our transcriptomic analysis and subsequent qPCR validation showed that overexpressing porcine IFI35 regulated the host innate immune response and elevated the transcription of genes *IFNB1*, *IFNE*, *MDA5*, *ISG15*, *OAS1* and *OAS2*. However, SIV infection significantly reduced these IFI35-induced regulations. NS1 of IAV employs multiple strategies to antagonize RLR signaling [30–32]. Our study confirms that SIV infection suppressed the transcription of endogenous IFI35, and its NS1 protein reduced the expression of the key RLR proteins MDA5, RIG-I, and MAVS. These findings reveal the strategy used by SIV NS1 to suppress the innate immune response triggered by porcine IFI35: SIV NS1 suppresses the pivotal signals of the RLR cascade, significantly reducing the protein levels of MDA5, RIG-I, and MAVS, thereby depleting key RLR signaling components required for the antiviral response. Notably, human IFI35 has been reported to engage in mutual antagonism with IAV NS1 through a direct protein–protein interaction [22]. Whether such a physical interaction also occurs between porcine IFI35 and H1N1 SIV NS1 remains to be confirmed in future studies. Collectively, our data indicate that SIV NS1 disrupts the RLR-MAVS signaling pathway upon which IFI35 relies to sustain its downstream antiviral activity.

While our study provides in vitro evidence of the IFI35-mediated antiviral bioactivity and its antagonism by NS1, certain limitations remain. First, all experiments relied on overexpression systems, which may not reflect endogenous IFI35 levels; second, only a single H1N1 SIV strain was tested; third, IFN-ε was assessed only at the transcriptional level. Future in vivo studies using gene-edited pigs are warranted to validate the physiological impact of porcine IFI35 on SIV pathogenesis. Furthermore, confirming whether porcine IFI35 physically interacts with SIV NS1, as well as comprehensively elucidating the mechanism by which porcine IFI35 activates the RIG-I-like receptor signaling pathway, is essential for further decoding the function of IFI35 during SIV infection.

5. Conclusions

In conclusion, our study provides insights into the interplay between porcine IFI35 and H1N1 SIV. Porcine IFI35 overexpression restricts H1N1 SIV replication and correlates with the upregulation of IFN-ε and several key downstream immune molecules. Additionally, we show that SIV NS1 antagonizes host RLR signaling by reducing MDA5, RIG-I, and MAVS protein levels and by suppressing IFI35-associated antiviral transcription. These findings characterize the antagonistic relationship between porcine IFI35 and SIV NS1 in host defense against SIV and highlight the complex antagonistic strategy of SIV NS1, providing potential targets for antiviral intervention.

Supplementary Materials: The following supporting information can be downloaded at: https://www.mdpi.com/article/10.3390/genes17111454/s1, Supplementary File S1: Table S1, Primer pairs used for quantitative RT-PCR analysis. Supplementary File S2: DEGs of transcriptome analysis. Supplementary File S3: GO enrichment analysis of transcriptome analysis. Supplementary File S4: Pathway enrichment analysis of transcriptome analysis.

Author Contributions: Conceptualization, S.Y.; methodology, Y.L. and Z.W.; validation, Y.L.; formal analysis, Y.L., Z.W. and S.Y.; investigation, Y.L.; resources, X.X. and S.Y.; data curation, Y.L.; writing—original draft, Y.L. and S.Y.; writing—review and editing, all authors; supervision, X.X. and S.Y.; project administration, X.X.; funding acquisition, Y.L. All authors have read and agreed to the published version of the manuscript.

Funding: This research was funded by the Science Research Project of Hebei Education Department (QN2024015), the National Key Research and Development Program of China (2023YFD1800704) and the Provincial Universities Basic Scientific Research Operating Expenses Special Project of Hebei Normal University of Science & Technology (2025JK007).

Institutional Review Board Statement: Not applicable.

Informed Consent Statement: Not applicable.

Data Availability Statement: The processed data supporting the findings of this study are available within the article and its Supplementary Materials. The raw sequence data reported in this paper have been deposited in the Genome Sequence Archive (Genomics, Proteomics & Bioinformatics 2025) in the National Genomics Data Center (Nucleic Acids Res 2025), China National Center for Bioinformation/Beijing Institute of Genomics, Chinese Academy of Sciences (GSA: CRA044838; BioProject accession PRJCA066881), and are publicly accessible at https://ngdc.cncb.ac.cn/gsa, accessed on 17 June 2028.

Conflicts of Interest: The authors declare no conflicts of interest. The authors further confirm that there are no personal circumstances or interests that may be perceived as inappropriately influencing the representation or interpretation of the reported research results. The funders had no role in the design of the study; in the collection, analyses, or interpretation of data; in the writing of the manuscript; or in the decision to publish the results.

Abbreviations

The following abbreviations are used in this manuscript:

IAV	Influenza A virus
SIV	Swine influenza virus
IFI35	Interferon-induced protein 35
ISG	Interferon-stimulated gene
MAVS	Mitochondrial antiviral-signaling protein
MDA5	Melanoma differentiation-associated protein 5
OAS	2′-5′-oligoadenylate synthetase
RIG-I	Retinoic acid-inducible gene I
IFN	Interferon
PRR	Pattern recognition receptor
TLR	Toll-like receptor
RLR	RIG-I-like receptor
MOI	Multiplicity of infection
$TCID_{50}$	Median tissue culture infectious dose
DEGs	Differentially expressed genes
GO	Gene ontology
KEGG	Kyoto encyclopedia of genes and genomes
SeV	Sendai virus
qPCR	Quantitative PCR
CPE	Cytopathic effects

References

1. Zeller, M.A.; Ma, J.; Wong, F.Y.; Tum, S.; Hidano, A.; Holt, H.; Chhay, T.; Sorn, S.; Koeut, D.; Seng, B.; et al. The Genomic Landscape of Swine Influenza a Viruses in Southeast Asia. *Proc. Natl. Acad. Sci. USA* **2023**, *120*, e2301926120. [CrossRef] [PubMed]
2. Novel Swine-Origin Influenza A (H1N1) Virus Investigation Team; Dawood, F.S.; Jain, S.; Finelli, L.; Shaw, M.W.; Lindstrom, S.; Garten, R.J.; Gubareva, L.V.; Xu, X.; Bridges, C.B.; et al. Emergence of a Novel Swine-Origin Influenza a (H1N1) Virus in Humans. *N. Engl. J. Med.* **2009**, *360*, 2605–2615. [CrossRef] [PubMed]

3. Ma, W. Swine Influenza Virus: Current Status and Challenge. *Virus Res.* **2020**, *288*, 198118. [CrossRef] [PubMed]
4. Pomorska-Mol, M.; Dors, A.; Kwit, K.; Czyzewska-Dors, E.; Pejsak, Z. Coinfection Modulates Inflammatory Responses, Clinical Outcome and Pathogen Load of H1N1 Swine Influenza Virus and *Haemophilus parasuis* Infections in Pigs. *BMC Vet. Res.* **2017**, *13*, 376. [CrossRef] [PubMed]
5. Iwasaki, A.; Pillai, P.S. Innate Immunity to Influenza Virus Infection. *Nat. Rev. Immunol.* **2014**, *14*, 315–328. [CrossRef] [PubMed]
6. Komadina, N.; McVernon, J.; Hall, R.; Leder, K. A Historical Perspective of Influenza A(H1N2) Virus. *Emerg. Infect. Dis.* **2014**, *20*, 6–12. [CrossRef] [PubMed]
7. Petro-Turnquist, E.; Pekarek, M.J.; Weaver, E.A. Swine Influenza a Virus: Challenges and Novel Vaccine Strategies. *Front. Cell Infect. Microbiol.* **2024**, *14*, 1336013. [CrossRef] [PubMed]
8. Liu, Y.; Olagnier, D.; Lin, R. Host and Viral Modulation of RIG-I-Mediated Antiviral Immunity. *Front. Immunol.* **2016**, *7*, 662. [CrossRef] [PubMed]
9. Streicher, F.; Jouvenet, N. Stimulation of Innate Immunity by Host and Viral RNAs. *Trends Immunol.* **2019**, *40*, 1134–1148. [CrossRef] [PubMed]
10. Blanco-Melo, D.; Nilsson-Payant, B.E.; Liu, W.C.; Uhl, S.; Hoagland, D.; Moller, R.; Jordan, T.X.; Oishi, K.; Panis, M.; Sachs, D.; et al. Imbalanced Host Response to SARS-CoV-2 Drives Development of COVID-19. *Cell* **2020**, *181*, 1036–1045.e9. [CrossRef] [PubMed]
11. Arilahti, V.; Makela, S.M.; Tynell, J.; Julkunen, I.; Osterlund, P. Novel Avian Influenza a (H7N9) Virus Induces Impaired Interferon Responses in Human Dendritic Cells. *PLoS ONE* **2014**, *9*, e96350. [CrossRef] [PubMed]
12. Park, A.; Iwasaki, A. Type I and Type III Interferons—Induction, Signaling, Evasion, and Application to Combat COVID-19. *Cell Host Microbe* **2020**, *27*, 870–878. [CrossRef] [PubMed]
13. Zhang, M.; Li, J.; Yan, H.; Huang, J.; Wang, F.; Liu, T.; Zeng, L.; Zhou, F. ISGylation in Innate Antiviral Immunity and Pathogen Defense Responses: A Review. *Front. Cell Dev. Biol.* **2021**, *9*, 788410. [CrossRef] [PubMed]
14. Perng, Y.C.; Lenschow, D.J. ISG15 in Antiviral Immunity and Beyond. *Nat. Rev. Microbiol.* **2018**, *16*, 423–439. [CrossRef] [PubMed]
15. Bange, F.C.; Vogel, U.; Flohr, T.; Kiekenbeck, M.; Denecke, B.; Bottger, E.C. IFP 35 Is an Interferon-Induced Leucine Zipper Protein That Undergoes Interferon-Regulated Cellular Redistribution. *J. Biol. Chem.* **1994**, *269*, 1091–1098. [CrossRef]
16. Wang, X.; Johansen, L.M.; Tae, H.J.; Taparowsky, E.J. IFP 35 Forms Complexes with B-ATF, a Member of the AP1 Family of Transcription Factors. *Biochem. Biophys. Res. Commun.* **1996**, *229*, 316–322. [CrossRef] [PubMed]
17. Zhou, X.; Liao, J.; Meyerdierks, A.; Feng, L.; Naumovski, L.; Bottger, E.C.; Omary, M.B. Interferon-Alpha Induces Nmi-IFP35 Heterodimeric Complex Formation That Is Affected by the Phosphorylation of IFP35. *J. Biol. Chem.* **2000**, *275*, 21364–21371. [CrossRef] [PubMed]
18. Das, A.; Dinh, P.X.; Panda, D.; Pattnaik, A.K. Interferon-Inducible Protein IFI35 Negatively Regulates RIG-I Antiviral Signaling and Supports Vesicular Stomatitis Virus Replication. *J. Virol.* **2014**, *88*, 3103–3113. [CrossRef] [PubMed]
19. Zheng, W.; Li, X.; Wang, J.; Li, X.; Cao, H.; Wang, Y.; Zeng, Q.; Zheng, S.J. A Critical Role of Interferon-Induced Protein IFP35 in the Type I Interferon Response in Cells Induced by Foot-and-Mouth Disease Virus (FMDV) Protein 2C. *Arch. Virol.* **2014**, *159*, 2925–2935. [CrossRef] [PubMed]
20. Tan, J.; Qiao, W.; Wang, J.; Xu, F.; Li, Y.; Zhou, J.; Chen, Q.; Geng, Y. IFP35 Is Involved in the Antiviral Function of Interferon by Association with the Viral Tas Transactivator of Bovine Foamy Virus. *J. Virol.* **2008**, *82*, 4275–4283. [CrossRef] [PubMed]
21. Zhang, X.; Zhang, Y.; Wei, F. Research Progress on the Nonstructural Protein 1 (NS1) of Influenza a Virus. *Virulence* **2024**, *15*, 2359470. [CrossRef] [PubMed]
22. Yang, H.; Winkler, W.; Wu, X. Interferon Inducer IFI35 Regulates RIG-I-Mediated Innate Antiviral Response through Mutual Antagonism with Influenza Protein NS1. *J. Virol.* **2021**, *95*, e00283-21. [CrossRef] [PubMed]
23. Wang, Z.; Ye, S.; Yao, C.; Wang, J.; Mao, J.; Xu, L.; Liu, Y.; Fu, C.; Lu, G.; Li, S. Antiviral Activity of Canine RIG-I against Canine Influenza Virus and Interactions between Canine RIG-I and CIV. *Viruses* **2021**, *13*, 2048. [CrossRef] [PubMed]
24. Abdelwhab, E.M.; Mettenleiter, T.C. Zoonotic Animal Influenza Virus and Potential Mixing Vessel Hosts. *Viruses* **2023**, *15*, 980. [CrossRef] [PubMed]
25. Cai, M.; Wei, Z.; Hu, X.; Ji, Y.; Li, S.; Huang, J.; Jin, R.; Liang, Q.; Zhang, G.; Zheng, Z.; et al. The Evolution, Complexity, and Diversity of Swine Influenza Viruses in China: A Hidden Public Health Threat. *Virology* **2024**, *598*, 110167. [CrossRef] [PubMed]
26. Szretter, K.J.; Gangappa, S.; Belser, J.A.; Zeng, H.; Chen, H.; Matsuoka, Y.; Sambhara, S.; Swayne, D.E.; Tumpey, T.M.; Katz, J.M. Early Control of H5N1 Influenza Virus Replication by the Type I Interferon Response in Mice. *J. Virol.* **2009**, *83*, 5825–5834. [CrossRef] [PubMed]
27. Sang, Y.; Rowland, R.R.; Hesse, R.A.; Blecha, F. Differential Expression and Activity of the Porcine Type I Interferon Family. *Physiol. Genom.* **2010**, *42*, 248–258. [CrossRef] [PubMed]
28. Sang, Y.; Bergkamp, J.; Blecha, F. Molecular Evolution of the Porcine Type I Interferon Family: Subtype-Specific Expression and Antiviral Activity. *PLoS ONE* **2014**, *9*, e112378. [CrossRef] [PubMed]
29. Zhao, F.R.; Wang, W.; Zheng, Q.; Zhang, Y.G.; Chen, J. The Regulation of Antiviral Activity of Interferon Epsilon. *Front. Microbiol.* **2022**, *13*, 1006481. [CrossRef] [PubMed]

30. Sha, T.W.; Weber, M.; Kasumba, D.M.; Noda, T.; Nakano, M.; Kato, H.; Fujita, T. Influenza a Virus NS1 Optimises Virus Infectivity by Enhancing Genome Packaging in a dsRNA-Binding Dependent Manner. *Virol. J.* **2020**, *17*, 107. [CrossRef] [PubMed]
31. Suleman, M.; Sayaf, A.M.; Khan, A.; Khan, S.A.; Albekairi, N.A.; Alshammari, A.; Agouni, A.; Yassine, H.M.; Crovella, S. Molecular Screening of Phytocompounds Targeting the Interface between Influenza a NS1 and TRIM25 to Enhance Host Immune Responses. *J. Infect. Public Health* **2024**, *17*, 102448. [CrossRef] [PubMed]
32. Lamotte, L.A.; Tafforeau, L. How Influenza a Virus NS1 Deals with the Ubiquitin System to Evade Innate Immunity. *Viruses* **2021**, *13*, 2309. [CrossRef] [PubMed]

Disclaimer/Publisher's Note: The statements, opinions and data contained in all publications are solely those of the individual author(s) and contributor(s) and not of MDPI and/or the editor(s). MDPI and/or the editor(s) disclaim responsibility for any injury to people or property resulting from any ideas, methods, instructions or products referred to in the content.